17th Australasian Fluid Mechanics Conference
Auckland, New Zealand
5-9 December 2010

An Assessment of Average Bubble Number Density Model for Bubbly Flows

S.C.P. Cheung[1], X.Y. Duan[1,2], G.H. Yeoh[3,4], J.Y. Tu[1], E. Krepper[5] and D. Lucas[5]

[1]School of Aerospace, Mechanical and Manufacturing Engineering
RMIT University, Melbourne, Victoria 3083, Australia

[2]Institute of Refrigeration and Cryogenic Engineering
Xi'an Jiaotong University, Xi'an 710049, China

[3]Australian Nuclear Science and Technology Organization
PMB 1, Menai, New South Wales 2234, Australia

[4]School of Mechanical and Manufacturing Engineering
University of New South Wales, Sydney, New South Wales 2052, Australia

[5]Institute of Safety Research
Forschungszentrum Rossendrof e.V., P.O. Box 510 119, 01314 Dresden, Germany

Abstract

Gas-liquid bubbly flows with wide range of bubble sizes are commonly encountered in many industrial applications. Based on our previous study, a generalized Average Bubble Number Density (ABND) model has been developed to model the dynamical changes of bubble size due to bubble coalescence and breakage mechanism. With the aim to asses the model performance, numerical studies have been performed to validate the model predictions against experimental data. Three experimental data [7,10,12] exhibiting totally different bubble size evolution trends were strategically selected for the present validation study. Numerical predictions were validated against measured results under three different experimental conditions. In general, predictions of the ABND model yield good agreement with experimental data. The encouraging results demonstrated the capability of the ABND model in capturing the changes of bubbles size due to bubble interactions and the transition from "wall peak" to "core peak" gas volume fraction profiles under various flow conditions. Merits and drawbacks of the ABND model for industrial application are also discussed.

Introduction

Complex gas-liquid bubbly flow structures are featured in many practical applications. Bubble column reactors, which purposefully promote large interfacial areas for gas-liquid mass transfer and efficient mixing for competing gas-liquid reactions, are extensively employed in the chemical, petroleum, mining and pharmaceutical industries. In the past decades, the population balance (PB) approach attracted considerably attention from researchers attempting to resolve the sophisticated evolution processes of gas-liquid flows [3,5]. An Averaged Bubble Number Density (ABND) model has been introduced as a compact and efficient population balance method to obtain engineering solutions for practical gas-liquid bubbly flows. Coalescence and breakage kernels proposed by Yao and Morel [14] was found to be the best candidate to model bubble coalescence and breakage phenomena in comparison to other mechanistic kernels by Wu et al. [14] and Hibiki and Ishii [6].

Nevertheless, as in other kernel developments, mechanistic kernels of Yao and Morel [15] was derived and calibrated against a set of experimental database. Six different bubbly flow conditions, including four subcooled boiling measurements of the DEBORA experiment and two isothermal bubbly flows of the DEDALE experiment were selected for model calibration. Both experiments were carried out in small diameter pipes (i.e. ranged from 19.2 mm to 38.1 mm) with bubble size ranging from 0.5 mm to 4 mm. In practical, large-scale industrial bubble columns with wider range of bubble size is commonly exist due to the large internal pipe diameter and rigorous breakage and coalescence processes. A more thorough assessment of the kernels in predicting the bubble size evolution under various flow conditions and larger pipe diameter is crucial to realize its potential for practical industrial applications.

In the present article, to explore the capability of ABND model and mechanistic kernels of Yao and Morel [15] in solving practical large scale bubbly flows, model predictions are strategically validated against three different experimental data [7,10,12] where three completely different bubble size evolution trends (i.e. coalescence dominant, breakage dominant and balance) were exhibited. Model predictions of some important parameters; such as: local volume fraction profile, bubble diameter and gas velocity; were assessed and validated against the experimental data. Performance of the kernels in capturing the dynamical bubble size changes within the system was also discussed

Mathematical Models

Based on our previous study [4], the two phase fluid motions are modeled through the two-fluid model based on Eulerian-Eulerian framework. In isothermal flow condition, with no interfacial mass transfer, the continuity equation of the two-phases is written as [8]:

$$\frac{\partial\left(\rho_i\alpha_i\right)}{\partial t}+\nabla\cdot\left(\rho_i\alpha_i\vec{u}_i\right)=0 \tag{1}$$

where α, ρ and $\vec{u}$ is the gas volume fraction, density and velocity of each phase. The subscripts *i=l* or *g* denotes the liquid or gas phase.

The momentum equation for the two-phase can be expressed as follow:

$$\frac{\partial\left(\rho_i\alpha_i\vec{u}_i\right)}{\partial t}+\nabla\cdot\left(\rho_i\alpha_i\vec{u}_i\vec{u}_i\right)=-\alpha_i\nabla P+\alpha_i\rho_i\vec{g}$$
$$+\nabla\cdot\left[\alpha_i\mu_i^e\left(\nabla\vec{u}_i+\left(\nabla\vec{u}_i\right)^T\right)\right]+F_i \tag{2}$$

On the right hand side of (2), F_i represents the total interfacial force calculated with averaged variables. Based on our previous study, interfacial drag and non-drag force models were adopted. Details of the model can be found in [4] and the references therein. $\vec{g}$ is the gravity acceleration vector and P is the pressure.

Average Bubble Number Density (ABND)

The Average Bubble Number Density (ABND) model as a simpler population balance approach is introduced to describe the bubble mechanism. The ABND transport equation based on the concept of population balance of dispersed bubbles is given by:

$$\frac{\partial n}{\partial t} + \nabla \cdot \left(\vec{u}_g n \right) = \phi_n^{RC} + \phi_n^{TI} \tag{3}$$

where n is the average bubble number density, φ_n^{RC} and φ_n^{TI} are the bubble number density changes due to random collision, turbulent induced breakage and wake entrainment respectively which is the key parts of describing bubble "birth" and "death" rate. For closure of the transport equation, coalescence and breakage kernels proposed by Yao and Morel [15] were adopted in the present study.

Yao and Morel [15] have pointed out that the aforementioned two models have been developed based on two different considerations: the free travelling time or the interaction time. They argued that both characteristic times are identically important. Taking two considerations into account, the bubble coalescence rate is derived as:

$$\phi_n^{RC} = -F_C C_{RC1} \frac{\alpha_g^2 \varepsilon^{1/3}}{D_S^{11/3}} \cdot \frac{\exp(-C_{RC2}\sqrt{We/We_{cr}})}{(\alpha_{\max}^{1/3} - \alpha_g)/\alpha_{\max}^{1/3} + C_{RC3}\alpha_g \sqrt{We/We_{cr}}} \tag{4}$$

where the derived coefficients are C_{RC1} = 2.86, C_{RC2} = 1.017 and C_{RC3} = 1.922.

The bubble breakage rate is given by:

$$\phi_n^{TI} = F_B C_{TI1} \frac{\alpha_g (1-\alpha_g) \varepsilon^{1/3}}{D_S^{11/3}} \cdot \frac{\exp(-We_{cr}/We)}{1 + C_{TI2}(1-\alpha_g)\sqrt{We/We_{cr}}} \tag{5}$$

where coefficients C_{TI1} =1.6 and C_{TI2} =0.42 are the derived model constants. F_C and F_b are the calibration factors for coalescence and breakage respectively. For the present study, F_C =0.05 and F_b=0.25 are specified for all experimental flow conditions.

Experimental Arrangements

As discussed in previous section, with the aim to assess the performance of ABND model in predicting large scale industrial column, three different experimental data exhibiting completely distinguished bubble size evolution trends were strategically selected for model validations. A brief discussion on the three experimental arrangements and its embedded physical phenomenon are here presented.

The two-phase flow experiment conducted by Hibiki et al. [7] was carried out in a round tube made of acrylic with an inner diameter (D) of 50.8 mm and a length (L) of 3061 mm. Air bubbles were introduced through a porous media with the pore size of 40μm by a compressor and premixed with the purified water in a mixing chamber before entering into the test section. The schematic diagram of the experimental arrangement is shown in Figure 1a.The temperature of the apparatus was kept at a constant temperature (20°C) within the deviation of ±0.2°C by a heat exchanger installed in a water reservoir. Local flow measurements using the double sensor and hotfilm anemometer probes were performed at three axial (height) locations of z/D = 6.0, 30.3 and 53.5 and 15 radial locations of r/R = 0 to 0.95. In this paper, numerical predictions have been compared against local measurements at two flow conditions: Case H1 with $\langle j_l \rangle$=0.491 m/s and $\langle j_g \rangle$=0.0556 m/s; Case H2 with $\langle j_l \rangle$=0.986 m/s and $\langle j_g \rangle$=0.113 m/s. The inlet void fractions are 5% and 10% respectively. The bubble size from the air injection is 2.5 mm for both cases.

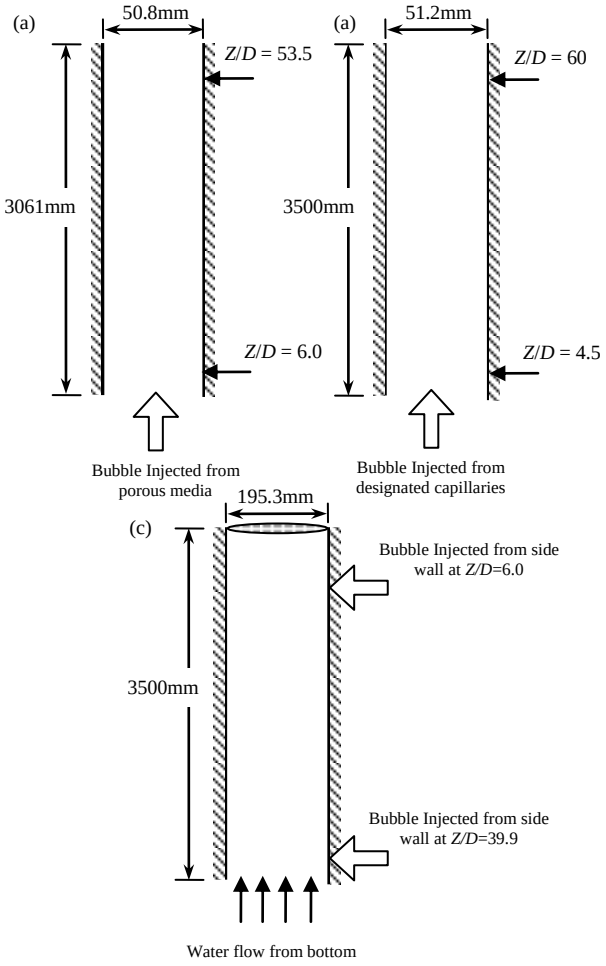

Z: The distance between measuring position and the gas injection units

Figure 1 Schematic diagram of experimental arrangement of (a) Hibiki et al. [7], (b) MTLOOP of Lucas et al. [10] and (c) TOPFLOW of Prasser et al. [12]

Figure 1b depicts the schematic diagram of the MTLOOP experiment designed by Lucas et al. [10]. Similar to the experiment by Hibiki et al. [7], gas-liquid bubbly flow was measured in a vertical medium size cylindrical pipe with a height of 3500 mm and an inner diameter of 51.2 mm. Water with a constant temperature of 30ºC was circulated from the bottom to the top of the pipe. Instead of porous media injection, air bubbles were injected via an injection device which consists of 19 capillaries with an inner diameter of 0.8 mm. These capillaries were equally distributed over the cross section area of the pipe. In order to measure the local instantaneous gas fraction void fraction as well as bubble size distribution, an electrode wire-mesh sensor is placed above a certain distance from the injection

device, which can be varied from 30 mm to 3030 mm (i.e. corresponding to dimensionless axial location Z/D = 0.6-60). For validations, two flow conditions were selected in this study: Case M1 with $<j_l>$=1.017 m/s and $<j_g>$=0.140 m/s; Case M2 $<j_l>$=1.017 m/s and $<j_g>$=0.219 m/s.

Schematic diagram of the large-scale TOPFLOW experimental facility of Prasser et al. [12] is shown in Figure 1c. A large vertical cylindrical pipe with the height 9000mm and inner diameter of 195.3mm inner diameter was adopted as test section. All measurements were performed at a nearly constant temperature of 30 °C with the deviations were no more than 1 °C. Different from previous bubbly flow experiments, a variable gas injection system was constructed by equipping with gas injection units at 18 different axial positions from Z/D=1.1 to Z/D=39.9. Air was injected through 72 annular distributed orifices of 1mm diameter. A fixed wire-mesh sensor was installed at the top of the pipe where instantaneous information of gas volume fraction and bubble size distribution was measured. Two flow conditions were selected for validation in this paper: Case T1 with $<j_l>$=0.641 m/s and $<j_g>$=0.219 m/s; Case T2 $<j_l>$=1.017 m/s and $<j_g>$=0.219 m/s.

Phenomenological Effects of Different Injection Methods

As different injection methods were adopted in the three experiments, a dimensional axial location (Z/D) is adopted to present the dimensional physical distance and bubbles size evolution between gas injection and measuring position within two different experiments. With the increase of Z/D, different trends of bubble coalescence and break-up were exhibited in the three experiments. In the TOPFLOW experiment, as high concentrated bubbles were injected at the side wall, large bubbles were formed via rapid coalescence of bubbles. These large bubbles were then interacted with turbulent eddies gradually collapsed to small bubble. Bubble size evolution was then governed by the breakage dominant phenomenon.

Bubble coalescence was found to be the dominant mechanism in the MTLOOP experiment. With air injection at the bottom, highly concentrated bubble and turbulent eddies were introduced into the system promoting more coalescence of bubbles. In contrast, coalescence and breakage were roughly in equilibrium in experiment of Hibiki et al. [7]. This could be caused by the pre-mixing effect of liquid and gas bubbles in mixing chamber which balances the bubble coalescence and breakage rate.

Numerical Modelling Details

The generic CFD code ANSYS CFX 11 (2007) was employed as a platform for two-fluid flow computation. The ABND model together with the coalescence and breakage kernels was implemented via the CFX Command Language (CCL) The Shear Stress Transport (SST) model [11] was adapted for liquid phase turbulence closure while the effect of bubbles on liquid turbulence was handled by the Sato's bubble-induced turbulent viscosity model. By assuming radial symmetry for all experiments, numerical simulations could be performed on a 60^o radial sector of the pipe with symmetry boundary conditions at both vertical sides. For the inlet boundary condition of Hibiki experiment, cross-section averaged gas void fraction, bubble size distribution and sauter mean bubble diameter which extracted from experimental data were specified. In accordance with the experiment arrangements, point sources were specified for the air injection in MTLOOP and TOPFLOW experiments.

Numerical Results Analysis

Figure 2 shows the predicted radial gas volume fraction distributions of the six selected flow conditions in comparison to the experimental data. The "wall peaking" profiles in Case H1 and H2 and the "Core peaking" profiles in Case M2, T1 and T2 were successfully captured by the model. In general, predictions are in good agreement with the measurements. Noticeable prediction errors were found for the Case M1. The transition profile from the "wall-to-core" peak was not appropriately captured and gas volume fraction at pipe centre was under-predicted. This could be attributed to the fact that the coalescence and breakage kernels slightly under-estimated bubble size to below 5.8mm (see also in Figure 3). In the present study, life force correlation of Tomiyama et al. [13] was adopted to handle the interfacial life force calculation. In agreement with experimental observation of Krepper et al. [9], the correlation prescribes that bubbles with diameter large than 5.8mm will be subjected to negative lift force forming a "core" peak profile and vice versa. As the bubble sizes were slightly under-estimated, gas volume fraction profiles were predicted as a "wall" peak distribution indeed. Moreover, in most of the test cases, gas volume fraction was over-predicted at the near wall region. This could be caused by the under-estimation of wall lubrication forces. In the present study, wall lubrication force model proposed by Antal et al. [1] and lift force model by Tomiyama [13] were adopted. Our predicted results revealed that the wall lubrication force is relatively weak in compared with the lift force which pushes small bubble toward near wall region. As a result, gas volume fraction was over-estimated.

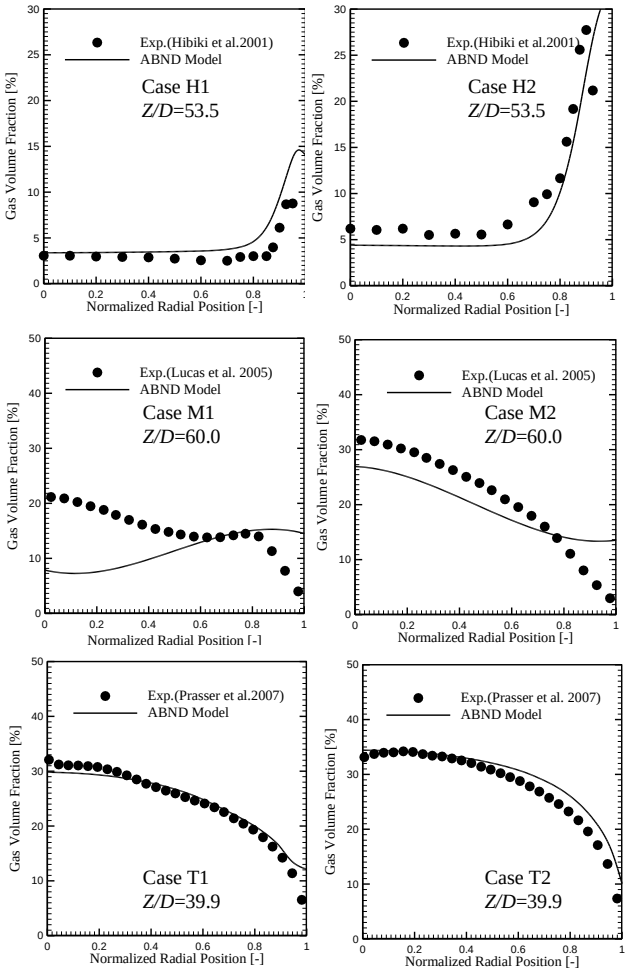

Figure 2 Comparison between predicted and measured radial gas volume fraction distribution for the six selected flow conditions of the three experiments

Comparison between predicted and measured bubble diameter in the six selected flow conditions is depicted in Figure 3. Radial bubble size distributions are shown for the Case H1, H2, T1 and T2. Due to the lack of measurements, cross-sectional averaged

bubble size profiles along the axial direction of the test section are given for the Case M1 and M2. Comparing the radial bubble size distributions, it can be observed that the trends of bubble size distributions were properly captured by the model. Bubble sizes were found to be over-predicted at the wall region in Case H1 and H2, while bubble sizes were under-estimated at the pipe core in Case T1 and T2. This reveals some plausible drawback of the model in accurately predict the detail bubble size evolution. Similarly, bubble sizes were also found under-predicted in Case M2. Nonetheless, the main trends of the bubble size evolution along the axial direction were successfully predicted in both cases (i.e. Case M1 and M2).

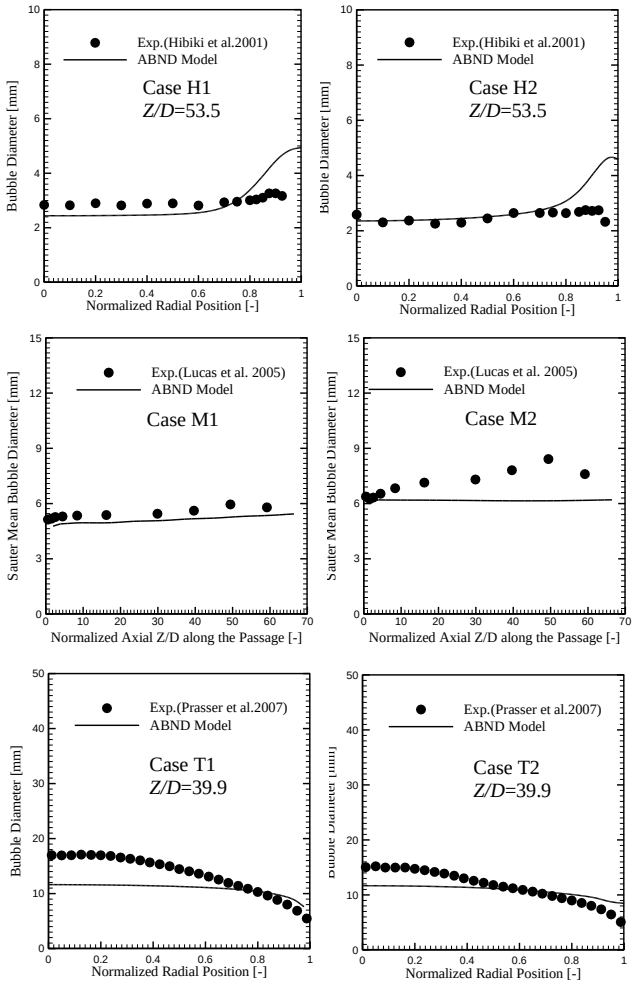

Figure 3 Comparison between predicted and measured bubble size distribution for the six selected flow conditions of the three experiments

Conclusions

A single averaged scalar population balance approach, namely Average Bubble Number Density (ABND) model, coupled with the Eulerian-Eulerian two-fluid model is presented in this paper to handle the various bubbly flows in isothermal condition. The ABND model incorporating with the coalescence and breakage mechanisms by Yao and Morel [15] were compared with six individual test cases of three different experiments with completely distinguished bubble size evolution trends. In general, the kernels gave satisfactory agreement with the gas volume fraction and bubble size diameter measurements. Although some noticeable prediction errors were found, with appropriate closure to model bubble breakup and coalescence mechanism, the ABND model is capable to project the main trend of bubble size changes throughout the entire system and provide solution of some important parameters; such as: local volume fraction profile and sauter mean bubble diameter, for practical engineering usage.

Acknowledgments

The financial support provided by the Australian Research Council (ARC project ID DP0877734) is gratefully acknowledged.

References

[1] Antal, S.P. Lahey Jr., R.T. & Flaherty, J.E., Analysis of phase distribution in fully developed laminar bubbly two-phase flow, *Int. J. Multiphase Flow*, **17**, 1991,635-652

[2] *CFX-11 User Manual*, ANSYS CFX, (2007).

[3] Chen, P. Dudukovic, M.P. & Sanyal, J., Three-dimensional simulation of bubble column flows with bubble coalescence and breakup, *AIChE J.*, **51**, 2005, 696-712.

[4] Cheung, S.C.P. Yeoh, G.H. & Tu, J.Y., On the numerical study of isothermal vertical bubbly flow using two population balance approaches. *Chem. Eng. Sci.*, **62**, 2007, 4659-4674.

[5] Ekambara, K., & Dhotre, M.T., Simulation of oscillatory baffled column: CFD and population balance, *Chem. Eng. Sci.*, **62**, 2007, 7205-7213.

[6] Hibiki, T. Ishii, M., One-group interfacial area transport of bubbly flows in vertical round tubes. *Int. J. Heat Mass Trans*, **43**, 2000, 2711-2726

[7] Hibiki, T. Ishii, M. & Xiao, Z., Axial interfacial area transport of vertical bubbly flows. *Int. J. of Heat Mass Trans.*, **44**, 2001, 1869-1888.

[8] Ishii, M., *Thermo-fluid dynamic theory of two-phase flow*, Eyrolles, Paris, 1975.

[9] Krepper, E. Lucas, D. Frank, T. Prasser, H.M. & Zwart, P.J., The inhomogeneous MUSIG model for the simulation of polydispersed flows, *Nucl. Eng. and Design*, **238**, 2008, 1690-1702.

[10] Lucas, D. Krepper, E. Prasser, H.M., Development of co-current air-water flow in a vertical pipe, *Int. J. of Multiphase Flow*, **31**, 2005, 1304-1328

[11] Menter, F.R., Two-equation eddy viscosity turbulence models for engineering applications, *AIAA J.*, **32**, 1994, 1598-1605.

[12] Prasser, H.M. Beyer, M. Carl, H. Gregor, S. Lucas, D. Pietruske, H. Schutz, P. & Weiss, F.P., Evolution of the structure of a gas-liquid two-phase flow in a large vertical pipe, *Nucl. Eng. and Design*, **237**, 2007, 1848-1861.

[13] Tomiyama, A., Struggle with computational bubble dynamics. In *Third International Conference on Multiphase Flow*, 1998, Lyon, France.

[14] Wu, Q. Kim, S. Ishii, M. & Beus, S.G., One-group interfacial area transport in vertical bubbly flow. *Int. J. Heat Mass Trans.*, **41**, 1998, 1103-1112

[15] Yao, W., Morel, C., Volumetric interfacial area prediction in upward bubbly two-phase flow, *Int. J. of Heat Mass Trans.*, **47**, 2004, 307-328